Heterogeneous integration of gallium nitride light-emitting diodes on diamond and silica by transfer printing

A. J. Trindade,[1,*] B. Guilhabert,[1] E. Y. Xie,[1] R. Ferreira,[1] J. J. D. McKendry,[1] D. Zhu,[2,3] N. Laurand,[1] E. Gu,[1] D. J. Wallis,[2,3] I. M. Watson,[1] C. J. Humphreys,[2] and M. D. Dawson[1]

[1]*Institute of Photonics, SUPA, University of Strathclyde, 106 Rottenrow, Glasgow G4 0NW, UK*
[2]*Department of Materials Science and Metallurgy, University of Cambridge, 27 Charles Babbage Road, Cambridge CB3 0FS, UK*
[3]*Plessey Semiconductors Ltd, Tamerton Road, Roborough, Plymouth, Devon, PL6 7BQ, UK*
[*]*antonio.trindade@strath.ac.uk*

Abstract: We report the transfer printing of blue-emitting micron-scale light-emitting diodes (micro-LEDs) onto fused silica and diamond substrates without the use of intermediary adhesion layers. A consistent Van der Waals bond was achieved via liquid capillary action, despite curvature of the LED membranes following release from their native silicon growth substrates. The excellence of diamond as a heat-spreader allowed the printed membrane LEDs to achieve optical power output density of 10 W/cm^2 when operated at a current density of 254 A/cm^2. This high-current-density operation enabled optical data transmission from the LEDs at 400 Mbit/s.

OCIS codes: (250.0250) Optoelectronics; (120.6810) Thermal effects; (060.4510) Optical communications.

References and links

1. H. S. Kim, E. Brueckner, J. Song, Y. Li, S. Kim, C. Lu, J. Sulkin, K. Choquette, Y. Huang, R. G. Nuzzo, and J. A. Rogers, "Unusual strategies for using indium gallium nitride grown on silicon (111) for solid-state lighting," Proc. Natl. Acad. Sci. U.S.A. **108**(25), 10072–10077 (2011).
2. T. Kim, S. Hyun Lee, Y. Li, Y. Shi, G. Shin, S. Dan Lee, Y. Huang, J. A. Rogers, and J. Su Yu, "Temperature- and size-dependent characteristics in ultrathin inorganic light-emitting diodes assembled by transfer printing," Appl. Phys. Lett. **104**(5), 051901 (2014).
3. J. Senawiratne, A. Chatterjee, T. Detchprohm, W. Zhao, Y. Li, M. Zhu, Y. Xia, X. Li, J. Plawsky, and C. Wetzel, "Junction temperature, spectral shift, and efficiency in GaInN-based blue and green light emitting diodes," Thin Solid Films **518**(6), 1732–1736 (2010).
4. Z. G. Ju, S. T. Tan, Z.-H. Zhang, Y. Ji, Z. Kyaw, Y. Dikme, X. W. Sun, and H. V. Demir, "On the origin of the redshift in the emission wavelength of InGaN/GaN blue light emitting diodes grown with a higher temperature interlayer," Appl. Phys. Lett. **100**(12), 123503 (2012).
5. Z. Gong, S. Jin, Y. Chen, J. McKendry, D. Massoubre, I. M. Watson, E. Gu, and M. D. Dawson, "Size-dependent light output, spectral shift, and self-heating of 400 nm InGaN light-emitting diodes," J. Appl. Phys. **107**(1), 013103 (2010).
6. S. Kim, J. Wu, A. Carlson, S. H. Jin, A. Kovalsky, P. Glass, Z. Liu, N. Ahmed, S. L. Elgan, W. Chen, P. M. Ferreira, M. Sitti, Y. Huang, and J. A. Rogers, "Microstructured elastomeric surfaces with reversible adhesion and examples of their use in deterministic assembly by transfer printing," Proc. Natl. Acad. Sci. U.S.A. **107**(40), 17095–17100 (2010).
7. E. James, Mark, Polymer Data Handbook, (Oxford University, 1999), pp. 424.
8. Z. L. Liau, "Semiconductor wafer bonding via liquid capillarity," Appl. Phys. Lett. **77**(5), 651 (2000).
9. D. Zhu, C. McAleese, K. K. McLaughlin, M. Häberlen, C. O. Salcianu, E. J. Thrush, M. J. Kappers, W. A. Phillips, P. Lane, D. J. Wallis, T. Martin, M. Astles, S. Thomas, A. Pakes, M. Heuken, and C. J. Humphreys, "GaN-based LEDs grown on 6-inch diameter Si (111) substrates by MOVPE," Proc. SPIE **7231**, 723118 (2009).
10. D. Zhu, C. McAleese, M. Haberlen, C. Salcianu, T. Thrush, M. Kappers, A. Phillips, P. Lane, M. Kane, D. Wallis, T. Martin, M. Astles, N. Hylton, P. Dawson, and C. Humphreys, "Efficiency measurement of GaN-based

#235263 - $15.00 USD Received 26 Feb 2015; revised 30 Mar 2015; accepted 30 Mar 2015; published 2 Apr 2015

quantum well and light-emitting diode structures grown on silicon substrates," J. Appl. Phys. **109**(1), 014502 (2011).
11. H. R. Shanks, P. D. Maycock, P. H. Sidles, and G. C. Danielson, "Thermal conductivity of Silicon from 300 to 1400°K," Phys. Rev. **130**(5), 1743–1748 (1963).
12. A. J. Trindade, B. Guilhabert, D. Massoubre, D. Zhu, N. Laurand, E. Gu, I. M. Watson, C. J. Humphreys, and M. D. Dawson, "Nanoscale-accuracy transfer printing of ultra-thin AlInGaN light-emitting diodes onto mechanically flexible substrates," Appl. Phys. Lett. **103**(25), 253302 (2013).
13. Y. Li, Y. Shi, J. Song, C. Lu, T. Kim, J. A. Rogers, and Y. Huang, "Thermal properties of microscale inorganic light-emitting diodes in a pulsed operation," J. Appl. Phys. **113**(14), 144505 (2013).
14. R. P. Mildren and J. R. Rabeau, Optical Engineering of Diamond, (Wiley-VCH, 2013), Ch. 2 and 11.
15. C. Kittel, "Interpretation of the thermal conductivity of glasses," Phys. Rev. **75**(6), 972–974 (1949).
16. J. J. D. McKendry, D. Massoubre, S. Zhang, B. R. Rae, R. P. Green, E. Gu, R. K. Henderson, A. E. Kelly, and M. D. Dawson, "Visible-light communications using a CMOS-controlled micro-light-emitting-diode array," J. Lightwave Technol. **30**(1), 61–67 (2012).
17. P. Tian, J. J. D. McKendry, Z. Gong, S. Zhang, S. Watson, D. Zhu, I. M. Watson, E. Gu, A. E. Kelly, C. J. Humphreys, and M. D. Dawson, "Characteristics and applications of micro-pixelated GaN-based light emitting diodes on Si substrates," J. Appl. Phys. **115**(3), 033112 (2014).
18. X. A. Cao, S. F. LeBoeuf, and T. E. Stecher, "Temperature-dependent electroluminescence of AlGaN-based UV LEDs," IEEE Electron Device Lett. **27**(5), 329–331 (2006).
19. MicroChem SU-8 Photoresists datasheet", http://www.microchem.com

1. Introduction

Transfer printing (TP) is a rapidly emerging technique for heterogeneous integration in electronics and optoelectronics [1–5]. In TP, soft elastomeric stamps are typically used to 'pick and place' device structures from their native growth substrate to a dissimilar receiving substrate, allowing the creation of novel hybrid device technologies. An important example of the application of this approach is in printing inorganic light-emitting diodes (LEDs), where pre-fabricated LED membrane devices can for example be transferred onto receiving substrates such as those based on polymers, enabling new forms of flexible displays [6]. As the technique matures and is optimized, thin membranes of suspended LED materials can be achieved in various ways, most commonly by directional wet etching of the growth substrate, here termed under-etching [1], or by laser lift-off [2]. However, a general issue for devices based on epitaxial multilayers is that removal of the substrate eliminates a natural heat-sink retained in conventional fabrication. This issue is severe for the important case of gallium nitride (GaN) based LEDs, in which, despite continuing efficiency improvements, most electrical input energy is dissipated as heat. Even for conventional devices in thermal contact with the growth substrate, operation under direct-current (dc) bias results in undesired thermal effects on the electroluminescence (EL), namely red spectral shifts and reduced optical output power (T-droop effect), while irreversible degradation of devices may also occur [3,4]. Reduction of the die size provides systematic improvement in heat dissipation, but does not eliminate these problems [5]. Heat dissipation from transfer-printed GaN-LEDs becomes a more pronounced issue when flexible polymeric materials are used as the receiver substrate, because these have lower thermal conductivities than inorganic materials used as the native growth substrate. Thermal effects in such a situation have been studied previously [2]. Regardless of the choice of receiver substrate in TP, the process flows normally feature adhesion-enhancement layers on the receiving substrates to aid the release of the LEDs from the transporting stamps [6]. Conventionally, these layers are organic materials, with poor thermal conductivities, κ (e.g. for polydimethylsiloxane (PDMS), κ ~0.15 W/m.K [7]). Therefore adhesion-enhancement layers impede heat dissipation from operating devices even if the underlying substrate has a relatively high thermal conductivity.

The attractive alternative to the use of a conventional adhesion-enhancement layer, which we report in this paper, is to use a transient layer of a volatile liquid [8]. The liquid film aids release of devices from the transporting stamps, as in a conventional process. Subsequently, capillary forces during evaporation of the liquid enable formation of a robust Van der Waals bond between the transferred devices and receiving substrate, with no permanent intermediate layer to add thermal resistance, or changes in refractive index, at the interfaces. This study

#235263 - $15.00 USD Received 26 Feb 2015; revised 30 Mar 2015; accepted 30 Mar 2015; published 2 Apr 2015

utilized high-performance GaN LED epistructures on Si (111) substrates [9,10]. While Si can act as a reasonably effective heat-sinking material in conventional devices (κ ~149 W/m.K [11]), this material is removed during the under-etching fabrication step, using potassium hydroxide (KOH) solution, needed in the TP process flow [12]. We compared two receiver substrates with thermal conductivities much higher and much lower than that of the GaN-based LED die (κ ~160 W/m.K for GaN [13]), namely diamond (κ ~2200 W/m.K [14]) and optical-grade silica glass (κ ~1.42 W/m.K [15]). The benefits of diamond as a heat spreader were investigated by comparing the dc characteristics of LEDs on these two receiver substrates. This part of our study included the use of thermal imaging to infer device operating temperatures, and to observe the transient heating effects under increasing dc drive currents. The ability of LEDs to operate at high dc current densities is also relevant to the emerging application of visible light communications (VLC) with LED sources [16]. In a typical situation where the data signal is superposed on a dc component, the modulation bandwidth of an LED increases with dc current up to a critical point [16,17]. As it is clearly of interest to see how transfer printed devices perform for VLC applications, we undertook comparison of the modulation bandwidths and data transmission characteristics of devices on diamond and silica.

2. Experimental results

We report the TP in array formats of 100x100 μm^2 LEDs (micro-LEDs) emitting around 465 nm onto single-crystal diamond platelets [14] (200 µm thick) and fused silica substrates (500 µm thick). We concentrate on LEDs of such small dimensions here by reason of applications described later in the paper, but note that scaling to larger areas [2] should in principle be possible if strain compensation issues specific to GaN/Si are addressed. The GaN micro-LED structures and process flow, together with the mechanical transfer system and PDMS stamps, are as described previously [12]. Here, however, capillary bonding was achieved by introducing an intermediate step to the TP process, in which the backside of the devices being transferred is wetted with a suitable liquid as shown in Fig. 1.

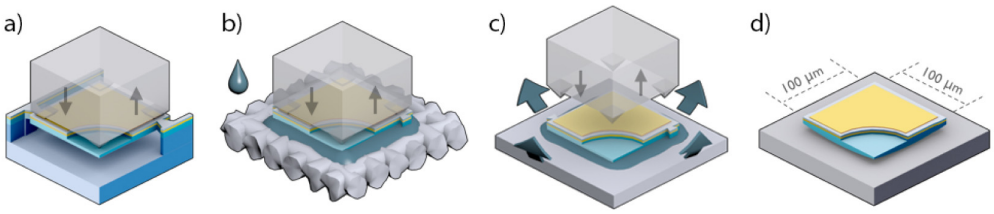

Fig. 1. Schematic of transfer printing using capillary bonding. The left-hand figure represents the pick-up of a suspended device using an elastomeric stamp (a). Upon pick-up, LEDs are compressed against an acetone-wetted cloth (b) and released when the backside contacts receiving substrate (c). The excess of liquid aids the positioning and release of the LED from the transporting stamp. After thermal curing, the LED is bonded to the new substrate (d).

After pick-up from the donor wafer as per Fig. 1(a), the backside is wetted on an acetone-impregnated standard cleanroom wipe as shown in Fig. 1(b). Quick retraction of the stamp removes the LED die from the wipe with its backside still wet, and it is then deposited onto the receiver substrate, shown in Fig. 1(c). The transparency of the stamps allows the TP process to be followed visually, and Fig. 2(a) confirms overflow of excess liquid to the sides of the LED die when it is compressed against the receiving substrate. Slow retraction of the stamp causes the liquid to partially reflow back underneath the die, and provide initial adhesion between the die and the receiving substrate, through liquid capillarity. This stage is shown in Fig. 2 (b). Subsequent evaporation of liquid proceeds from the outside of the die, and during this step the forces at the retreating meniscus bring the two surfaces into intimate contact [8]. While no specific tests have been performed at this time to assess the placement

#235263 - $15.00 USD Received 26 Feb 2015; revised 30 Mar 2015; accepted 30 Mar 2015; published 2 Apr 2015

accuracy in detail, the LEDs are printed using the same mechanical system we have previously shown to be capable of sub-micrometer placement [12], and we note that the printed dies hold their positioning during slow stamp retraction and later after the solvent has been evaporated.

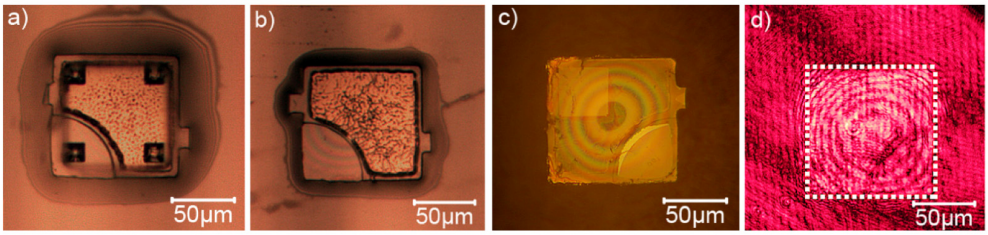

Fig. 2. Images illustrating the process of capillary bonding of individual LEDs onto rigid substrates. Parts (a) and (b) are optical microscope views through the transparent stamp at successive stages: (a) after wetting of the LED backside, contact is made with the receiving substrate; (b) stamp retraction allows the liquid to reflow underneath the LED. Parts (c) and (d) are views through the substrate showing interference effects from an air gap left round after liquid evaporation and bonding in the central region: (c) colored fringes visible under white light; (d) fringes observed under laser light.

After moderate heating to 50°C to evaporate any remaining liquid, the devices are left bonded by Van der Waals forces over the contact area with the receiving substrate. Both combinations of surfaces brought into contact (i.e. diamond or silica substrates, and the micro-LED backside) display similar root-mean-square roughness values of ~1 nm as measured by atomic force microscopy (AFM). We have previously attributed the smoothness of the micro-LED bonding surface to a protective SiN_x layer formed between the Si substrate and the AlN growth initiation layer [17]. This layer can largely protect the underside of the III-nitride die from attack by the KOH etch solution used to remove the Si substrate. Such low roughness results in two tightly-bonded surfaces robust to mechanical disturbance, and surviving multiple wet-processing steps necessary to complete the device fabrication. However, imaging of the devices through the back of the receiving substrate reveals a pattern of interference rings associated with an air gap as shown in Fig. 2(c) and 2(d). This observation correlates with curvature of the LED dies, which limits contact to the central region of the LED. Such curvature is reasonable to expect after removal of the Si substrate beneath the LED epistuctures. The epistructures are engineered such that the total epi-layer/Si substrate system is approximately strain balanced. This requires compressive strain to be introduced into the AlGaN buffer layers using lattice mismatch to counteract the tensile strain introduced by the thermal expansion difference between the nitride layers and the Si substrate on cooling from the growth temperature. After removal of the Si substrate this residual compressive strain in the AlGaN buffer layers then induces the concave curvature seen, as it acts against the topmost GaN layers in the LED stack.

The method to investigate the observed curvature of the LED dies after deposition used the imaged interference rings under monochromatic and coherent (653nm-emitting laser diode) light, exemplified in Fig. 2(d), and standard analysis of optical interference. The height of the die-substrate air gap was spatially reconstructed, allowing visualization of the backplane curvature over a full die as illustrated in Fig. 3(a). Essential information regarding the die positioning and tilting can be obtained from such measurements. The effective contact area, corresponding to the colorless mesh in Fig. 3(a), in the central region of a sample LED was found to be 14 ± 2% of the total die area and a radius of curvature averaging 2 mm per die (assuming a spherical curvature).

#235263 - $15.00 USD Received 26 Feb 2015; revised 30 Mar 2015; accepted 30 Mar 2015; published 2 Apr 2015

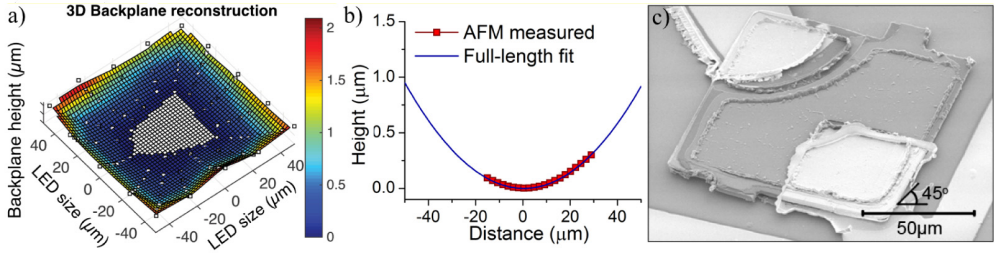

Fig. 3. Backplane curvature measurements. In (a), the calculated height of the air gap between a bonded LED and the substrate is represented as a mesh reconstructed by the photographed interference pattern. The colorless central area indicates where contact is assumed to occur. In part (b), an AFM line scan over the central area of an unbonded LED die is shown and extrapolated with a parabolic fit. Part (c) shows an SEM image of a micro-LED transfer printed onto a rigid substrate (at 45° tilt), and connected to Ti/Au metal tracks.

To further analyze the backplane curvature, an AFM profile scan was performed (45μm in length) on a flipped-over die where the central area was measured and fitted over the entire lateral size of the die as shown in Fig. 3(b). By zeroing the measurement to the minimum height as the center of the backplane curvature, the AFM height scan matches the interference rings height reconstruction for the area surrounding the center of the die (with ± 2 μm lateral fluctuations). However - towards the edges of the reconstructed backplane - higher curvature zones can be seen as per Fig. 3(a), indicating that the radius of curvature is not constant. SEM imaging provided a qualitative assessment of the height at the extremities of ~2.5 μm closely matching the values attained by the interference-based measurements.

To act as an electrical insulation layer and encapsulation for the devices on diamond and silica receiver substrates, an SU-8 epoxy photoresist layer of 10 μm post-cure thickness was deposited and patterned. Metal tracks, comprising 200 nm of Au above 50 nm of Ti, were deposited next, contacting the LED through localized apertures in the SU-8. The media surrounding LED dies in such a situation are shown in the right-hand part of Fig. 4(a).

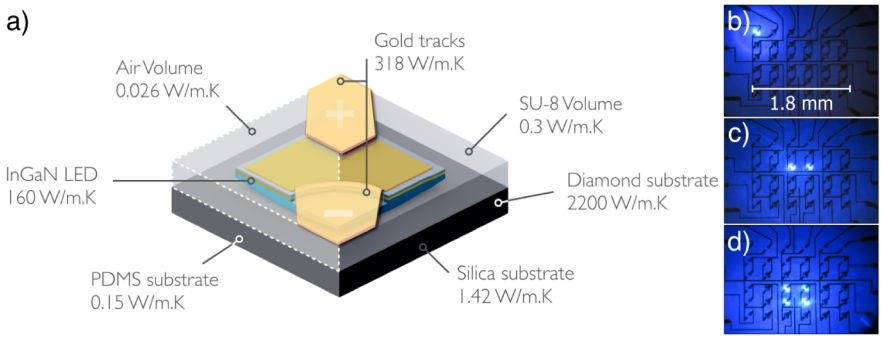

Fig. 4. Thermal conductivities of media surrounding the respective transfer-printed LEDs (a): The left half-section of the device illustrates the air-exposed baseline devices deposited on PDMS adhesion enhancement layers. The right half-section represents the case of the better performing substrates (diamond and silica) with improved heat dissipation and volumetric SU-8 (κ ~0.3 W/m.K [19]) encapsulation on top. Full device arrays can be seen in the microscope images in parts (b), (c) and (d) with configurations of 1, 2 and 4 active LEDs respectively.

As well as introducing the capillary-assisted TP of LEDs onto diamond and silica, we also fabricated for reference identical device structures onto PDMS/polyethylene terephthalate (PET) flexible substrates as previously demonstrated [17]. The media surrounding dies in this case are shown in the left-hand part of Fig. 4(a). 6x6 device arrays were assembled onto each substrate with alternative LED driving configurations as pictured in Fig. 4(b)-(d).

#235263 - $15.00 USD Received 26 Feb 2015; revised 30 Mar 2015; accepted 30 Mar 2015; published 2 Apr 2015

Figure 5 shows the operating voltage (V) and the optical output power density (L) of three representative LEDs as a function of the current density (J). L-J curves were acquired with the devices in direct contact with a calibrated Si photodiode detector, capturing only the light going through the supporting substrate. Characteristics of a reference micro-LED bonded to a PET polymer substrate with a 20-μm PDMS intermediate adhesion layer are included for comparison with those of the devices on diamond and bulk silica substrates. The devices on the PDMS/PET substrates were in direct thermal contact with air on one side, while those bonded to the inorganic receiver substrates were encapsulated with SU-8 epoxy as described above. The reference devices operated at a maximum drive current density of 30 A/cm^2, producing an optical output power density of 55 mW/cm^2 before permanent damage was observed. This limited performance is attributable to a poor environment for heat dissipation. The media on opposite sides of the LED dies, air and PDMS, both have lower thermal conductivities than their counterparts in the encapsulated devices bonded to inorganic substrates. LEDs on all three substrates display similar turn-on voltages (~4.5 V), indicating good ohmic contacts, and effective performance from the thin metal current-spreading layer over the p-GaN. A maximum current density of 255 A/cm^2 was measured without significant thermal roll-over on diamond substrates, representing a major improvement when compared to similar devices on soft intermediate layers (~30 A/cm^2) [2,12] .

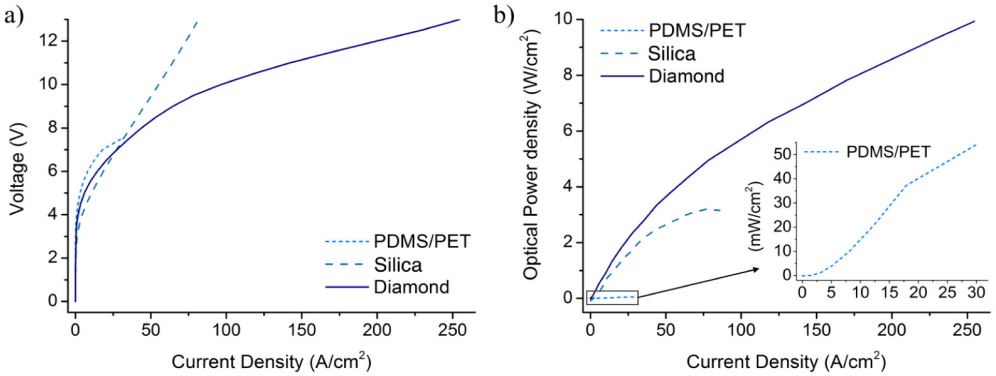

Fig. 5. Characteristics of an individual LED in operation on different substrates. In (a), J-V curves for individual LEDs on PDMS/PET, silica and diamond substrates, respectively. In (b) the corresponding L-J with the inset showing a magnification of the device emission on the PDMS/PET substrates used as a baseline comparison achieving a maximum optical power density of 55 mW/cm^2.

The maximum values for optical power density in Fig. 5 for devices on inorganic receiver substrates were 10 W/cm^2 at 255 A/cm^2 (I = 20 mA) and 3.2 W/cm^2 at 77 A/cm^2 (I = 6 mA) for devices on diamond and silica respectively. LEDs on silica gave a maximum optical power inferior to their counterparts on diamond, and started to reach saturation from thermal rollover after 78 A/cm^2. However, repeated drives up to 80 A/cm^2 showed no damage to the LEDs, in contrast to the irreversible damage suffered by devices on PDMS/PET above 30 A/cm^2. LEDs on diamond consistently outperformed those on the other substrates, due to its orders of magnitude higher thermal conductivity. The maximum optical power density *per* LED (10 W/cm^2) was nearly three times higher than that obtained from devices on silica. This represents a significant advance, outperforming previously reported transfer-printed devices with an equal die size by a factor of 10 [2].

To better understand how the two very different thermal conductivities of diamond and silica affected the device performance, the temperature distribution across LED arrays was measured with a calibrated thermal infrared camera, viewing through the substrate [Fig. 6(a)] and focusing on the plane of the LEDs. The camera acquisitions accounted for the emissivity of the GaN in the wavelength range of 1.5 to 5μm and the false-color representation of

#235263 - $15.00 USD Received 26 Feb 2015; revised 30 Mar 2015; accepted 30 Mar 2015; published 2 Apr 2015

temperature is referenced to the emissivity of GaN. The images show semi-quantitatively the much greater effectiveness of heat spreading in the array on diamond. At the highest current density no hot spots are evident, in contrast to the hot spot around the powered LED on glass, and there is a comparable temperature rise across the full diameter (3 mm) of the diamond substrate.

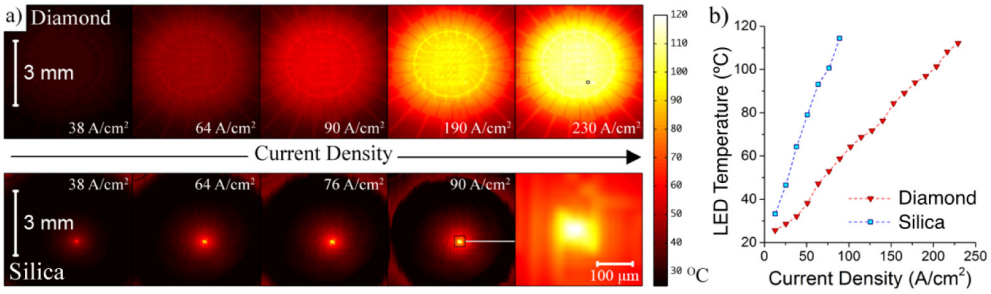

Fig. 6. (a) Thermal imaging of LED arrays with a single device powered on diamond (top) and silica (bottom). The emitting LED is identified in the last diamond frame as a black dot. The last frame of the silica-substrate row shows a magnified view of the die and its metal interconnection tracks. The captured images show the measured temperature corrected for the LED material (GaN); the rest of the image should be interpreted as a relative comparison. Part (b) shows the dependence of LED temperature on the injected current density (see Media 1).

Figure 6(a) also suggests the apparently enhanced temperature rise along the metal interconnection tracks. This is considered to be mainly an artifact arising from the metal emissivity and the calibration procedure, although a significant role for aluminum interconnection tracks in lateral heat transport in similar LED arrays has been proposed and simulated previously [1]. Figure 6(b) shows estimates of the temperature of the powered LED die as a function of drive current density for the two substrates, and shows an approximate linear dependence in each case. Devices are estimated to reach a maximum operating temperature of ~115°C. This is reached by devices on silica at an injection current density of 90 A/cm^2. LEDs on diamond attain a similar temperature only at 230 A/cm^2, a current density 2.5x higher. Representative heat-propagation visualization is available (see Media 1) showing real-time heat propagation with 1mA current increments on both substrates.

The very different heat-spreading properties of diamond and silica are expected to affect the spectral shifts shown by LEDs operating at different dc drive currents. Therefore electroluminescence spectra were recorded with a fiber-coupled spectrometer. Figure 7 shows how the peak EL wavelength shifted, and the inset illustrates typical spectra at relatively low current density. The peak EL emission of the transfer-printed devices shifted over a full range of 464 to 455 nm ($\Delta\lambda$ = 9 nm) and of 463 to 459 nm ($\Delta\lambda$ = 4 nm) on diamond and silica, respectively. The corresponding injected current densities ranged from 12 to 100 A/cm^2 for silica, and to a maximum of 256 A/cm^2 for diamond. In the case of LEDs on silica, the peak wavelength blue-shifts initially, with a reversal to a red shift above 50 A/cm^2 as similar to other reports of InGaN/GaN based LEDs [8]. The blue shift in polar (0001)-oriented device structures, as used here, are usually attributed to carrier screening by piezoelectric fields in the quantum well (QW) active region. Localized heating meanwhile causes strong competitive red shift effects - including bandgap shrinkage - which become dominant at higher injected current densities [8] and due to the devices own self-heating effects [10].

#235263 - $15.00 USD Received 26 Feb 2015; revised 30 Mar 2015; accepted 30 Mar 2015; published 2 Apr 2015

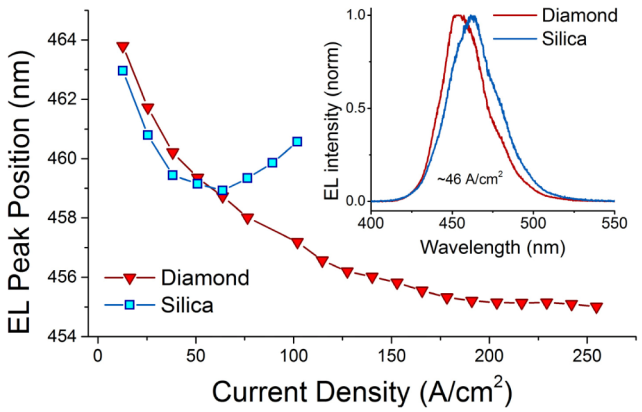

Fig. 7. EL peak shift of a representative single LEDs as a function of increasing injected current on diamond (red triangles) and silica (blue squares). The inset shows representative EL spectra at 46 A/cm2 for both substrates.

In the case of LEDs on diamond, a continuous blue shift is the net observable trend. Because these devices reached similar temperatures to those on silica at the highest current densities, the bandgap shrinkage contribution will be similar. It is likely that strain effects in the QWs, associated with thermal expansion mismatches between the III-nitride dies and underlying substrate, play a role in the markedly different spectral shift behavior [9]. The transition observed from initial blue shifts to red shifts parallels several previously published reports, which discuss contributing mechanisms in more depth, and their investigation with a wide range of techniques [2–4,18].

The combination of LED die sizes 10-100 times smaller in area than those of typical commercial GaN-based devices, and the ability to sustain high dc current densities through effective heat dissipation on diamond, motivated further fast-modulation measurements relevant to visible light communications (VLC) applications. A key parameter for VLC is the electrical-to-optical (E-O) modulation bandwidth (BW), which is conventionally measured using a −3 dB criterion. A small LED size naturally enhances BW by minimization of capacitive contributions, but a decrease in the differential carrier lifetime in GaN-based QWs as carrier density rises also gives a significant increase in BW with current density [16]. BW measurements on transfer-printed devices were acquired in a similar fashion to that reported elsewhere, applying a modulation signal on a constant dc bias [16]. Figure 8 shows the expected initial increase of BW with current density for devices on both diamond and silica.

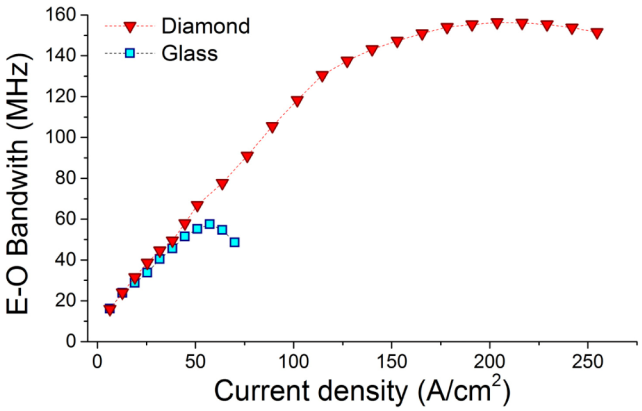

Fig. 8. E-O bandwidths as a function of dc drive current density of representative LEDs deposited onto diamond and silica.

#235263 - $15.00 USD Received 26 Feb 2015; revised 30 Mar 2015; accepted 30 Mar 2015; published 2 Apr 2015

Devices on both silica and diamond displayed similar performance for current densities under 50 A/cm^2. Above this point roll-over became evident for devices on silica, which are thus limited to a maximum BW of ~55 MHz. The BW of devices on diamond continued to increase at much higher current densities, and to plateau at 200 A/cm^2, corresponding to a maximum BW of 154 MHz. These maximum observed BW values, which establish a performance benchmark for transfer printed devices for optical communications, that could be further improved by fabricating smaller LEDs for use in the TP process. Interesting comparisons can also be made between the results in Fig. 8, and previous BW measurements on micro-LEDs fabricated from similar epitaxial material, but tested on the Si growth substrate [17]. These were circular in shape, and of 45 μm diameter. The previous non-transferred devices attained BWs of 190 MHz at relatively low current densities around 6 A/cm^2. However, they displayed an unusual temporary saturation of bandwidth increase in this current density range, before moderate further BW increases at higher current densities attributed to heating effects, and associated lowering of series resistance [17]. The smoother initial BW increase with current density shown by the transfer-printed devices resembles typical results from conventional GaN-on-sapphire devices [16]. These observations suggest that alteration of the strain state of QWs by removal of the Si substrate may influence the recombination dynamics of carriers significantly.

To further demonstrate the potential of the transfer-printed devices for VLC, tests were made of the optical transmission of data in a back-to-back configuration. The resulting eye diagrams are shown in Fig. 9. A simple on-off keying modulation scheme was used with a dc bias for the device on diamond of 10.5 V, and of 5.7 V for the device on the silica. A peak-to-peak modulation of 2 V was used in both configurations, and pseudo-random sequences of 2^7-1 bits were employed, as in previous work [16].

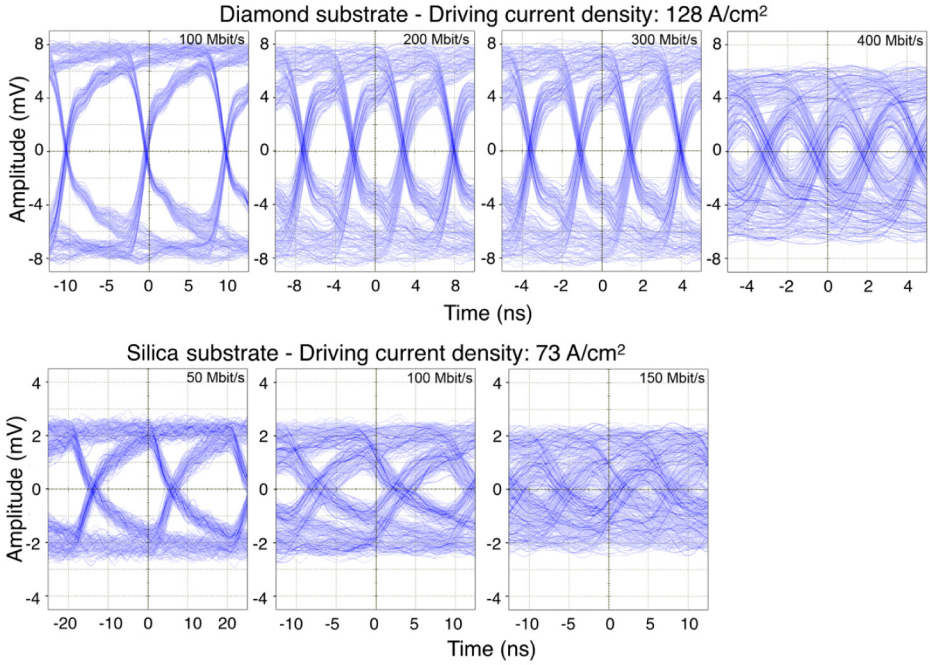

Fig. 9. Data-transmission measurements from representative LEDs deposited onto diamond (top row) and silica (lower row). The eye diagrams were acquired with the same dc applied current throughout.

Devices on diamond displayed open eye diagrams at data-rates up to 400 Mbit/s, correlating with error-free data transmission. In contrast, devices on silica showed eye closure

#235263 - $15.00 USD Received 26 Feb 2015; revised 30 Mar 2015; accepted 30 Mar 2015; published 2 Apr 2015

above 100 Mbit/s, which was virtually complete at 150 Mbit/s. The superior performance of the devices on diamond is again ultimately attributable to this material's effectiveness as a heat spreader, allowing operation of the LEDs at higher dc current densities.

3. Summary

Micro-transfer printing combined with liquid capillary bonding is demonstrated as a technique to directly integrate active device membranes to novel rigid substrates without adhesive interlayers. The technique retains the scalability and potentially nanometer positioning accuracy we have demonstrated previously [12], but brings additional benefits in direct contact to functional substrates including those possessing high thermal conductivity. As an important example of the use of this technique, the electrical and optical characteristics of 100 x 100 μm^2 blue-emitting GaN LEDs transfer printed in array format onto diamond and silica receiver substrates are compared, and demonstrate the major benefits of diamond as a heat-spreading material. Devices on diamond were driven at dc current densities up to 254 A/cm^2 without reaching thermal roll-over, or suffering permanent damage. A maximum optical output power density of 10 W/cm^2 was recorded from devices on diamond substrate, which is more than three times the optical power density of counterpart devices on silica (3.2 W/cm^2). The response of the devices to fast modulation, involving superposition of a data signal on a dc offset, was also studied, motivated by applications in optical data transmission. The effective heat dissipation offered by diamond allowed devices to attain maximum electrical-to-optical modulation bandwidths of 154 MHz at dc current densities of ~200 A/cm^2. The same devices achieved a highly competitive back-to-back data transmission rate of 400 Mbit/s at a dc current density of 128 A/cm^2.

The LED structures used in this study were optimized for conventional large-area LED fabrication, where the wafer-scale properties are most important. In future studies we will investigate how the strain profile in the layer stack can be modified to reduce the curvature of the micro-LEDs and improve the contact area, which should bring further benefits to the optoelectronic performance of the devices. We note finally that our technique of LED transfer printing onto diamond has the potential to take advantage of commercial-scale polycrystalline diamond substrates or the cost-economies to be expected from scaled up single-crystal CVD growth of diamond.

Acknowledgments

The authors thank Dr. P.R. Edwards, University of Strathclyde Department of Physics, for his assistance in the SEM imaging acquisition, and Dr. Anthony Kelly and Scott Watson, University of Glasgow, for support in the data transmission and bandwidth measurements. This work was supported by EPSRC grants EP/K00042X/1, EP/I029141/1, EP/F05999X/1, and EP/I012591/1.

#235263 - $15.00 USD Received 26 Feb 2015; revised 30 Mar 2015; accepted 30 Mar 2015; published 2 Apr 2015